Title	Fermi surface and magnetism of rare earth metal europium for α=2/3, 0.8, 0.9 and 1
Sub Title	
Author	福地, 充(Fukuchi, Mitsuru) 松本, 紳(Matsumoto, Makoto) 柴田, 郁子(Shibata, Ikuko) Sakiji, Yukihiro(Kobayashi, Shoichi) 小林, 正一
Publisher	慶応義塾大学工学部
Publication year	1980
Jtitle	Keio engineering reports Vol.33, No.7 (1980. 5) ,p.83- 95
JaLC DOI	
Abstract	Calculations are made for the band structure and for the detailed form of the Fermi surface of bcc Eu by the KKR (Green's function) method by using the exchange potential of α=2/3, 0.8, 0.9, in addition to α=1. Our purpose is to make clear from the theoretical standpoint the origin of the phenomena of helical spin ordering, which has been found below TN=91K by the neutron diffraction experiment. Among our results, a stress is made on the role of electron Fermi surface around H-point.
Notes	
Genre	Departmental Bulletin Paper
URL	https://koara.lib.keio.ac.jp/xoonips/modules/xoonips/detail.php?koara_id=KO50001004-00330007-0083

KEIO ENGINEERING REPORTS
VOL. 33, NO. 7, pp. 83-95, 1980

FERMI SURFACE AND MAGNETISM OF RARE EARTH METAL EUROPIUM FOR $\alpha=2/3$, 0.8, 0.9 AND 1

MITSURU FUKUCHI, MAKOTO MATSUMOTO, IKUKO SHIBATA,

Department of Instrumentation Engineering, Keio University, Hiyoshi, Yokohama 223, Japan

YUKIHIRO SAKIZI, AND SYO-ITI KOBAYASI

Physics Department, Nihon University, Sakurajosui-3, Setagaya, Tokyo 156, Japan

(Received 12 February 1980)

ABSTRACT

Calculations are made for the band structure and for the detailed form of the Fermi surface of bcc Eu by the KKR (Green's function) method by using the exchange potential of $\alpha=2/3$, 0.8, 0.9, in addition to $\alpha=1$. Our purpose is to make clear from the theoretical standpoint the origin of the phenomena of helical spin ordering, which has been found below $T_N=91$ K by the neutron diffraction experiment. Among our results, a stress is made on the role of electron Fermi surface around H-point.

§ 1. Introduction

As is well known, in the rare earth series, the number of 4f-electrons runs from zero at La to fourteen at Lu. Among these metals, Eu($4f^7 6s^2$) with a half-filled shell and Yb($4f^{14} 6s^2$) with a full shell appear in the divalent and cubic form, although almost all of the other rare-earths show the trivalent and hexagonal forms. On this account, it is rather surprizing that bcc Eu at low temperatures shows a helical spin ordering (HSO) which seems to be typical for the heavy rare earth metals Tb, Dy, Ho, Er, and Tm which all have hexagonal close-packed (hcp) structure commonly.

In the first-half of the 1960's NERESON et al. (1962; 1964) carried out neutron diffraction experiments by using samples in the form of Eu-filings, and proposed an HSO-model in which the spins lie parallel to the cube face and the spin rotation-axis is directed perpendicular to the spins below the Néel temperature $T_N=91$ K, and the period of the helix is $3.6a$ at a helium-temperature and changes very slightly with temperatures, where a is the lattice constant (the length of

the cubic unit-cell). The saturated ordered moment was observed as $5.9\pm0.4\ \mu_B$ per atom which is somewhat less than the theoretical value of $7\mu_B$ for Eu^{2+} in the ${}^8S_{7/2}$ state.

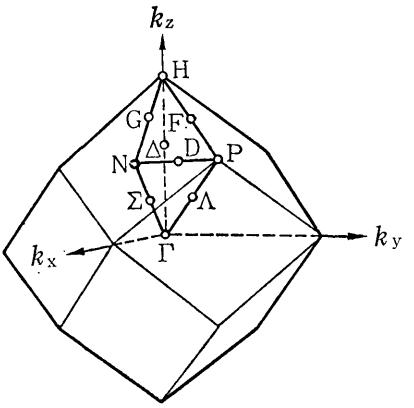

Fig. 1. bcc Brillouin zone (BZ) and its 1/48.

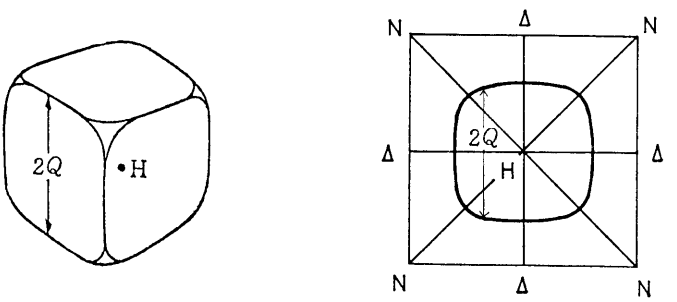

(a) (b)

Fig. 2. (a) Andersen and Loucks' electron Fermi surface around H ("superegg"). (b) Its cross-section in the HΓN-plane.

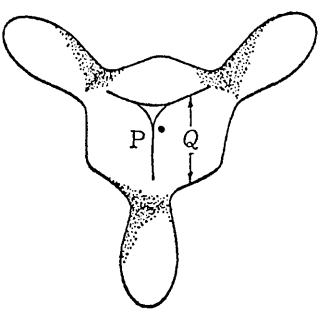

Fig. 3. Andersen and Loucks' hole Fermi surface around P ("tetracube").

On the other hand, the calculation of the energy band structure has been worked by FREEMAN and DIMMOCK (1966) and ANDERSEN and LOUCKS (1968), both by using the augmented plane wave (APW) method. Especially the latter authors aimed to derive the observed pitch wave-vector Q of the HSO by the nesting of portions of the Fermi surface. They have calculated the Fermi surface shape carefully and found that the surface consists of two pieces: an electron surface (called "superegg") around H-point which has a shape of rounded-off cube, and a hole surface (called "tetracube") around P-point which has also a shape of rounded-off cube attached by rather large ellipsoids stretching towards the four H-points. (As for H and P, see Fig. 1.) The "superegg" and its cross-section in the HΓN-plane [(100)-plane] are shown in Fig. 2, and the "tetracube" in Fig. 3.

ANDERSEN and LOUCKS (1968) have attributed the origin of the HSO to the nesting of the opposing faces of nearly cubic part of the "tetracube", because the corresponding Q-vector explains very well the observed helix both in direction and in magnitude of the period.

Though, in ANDERSEN and LOUCKS' Fermi surfaces, "superegg" and "tetracube" resemble each other in shape, the former seems to be more cube-like than

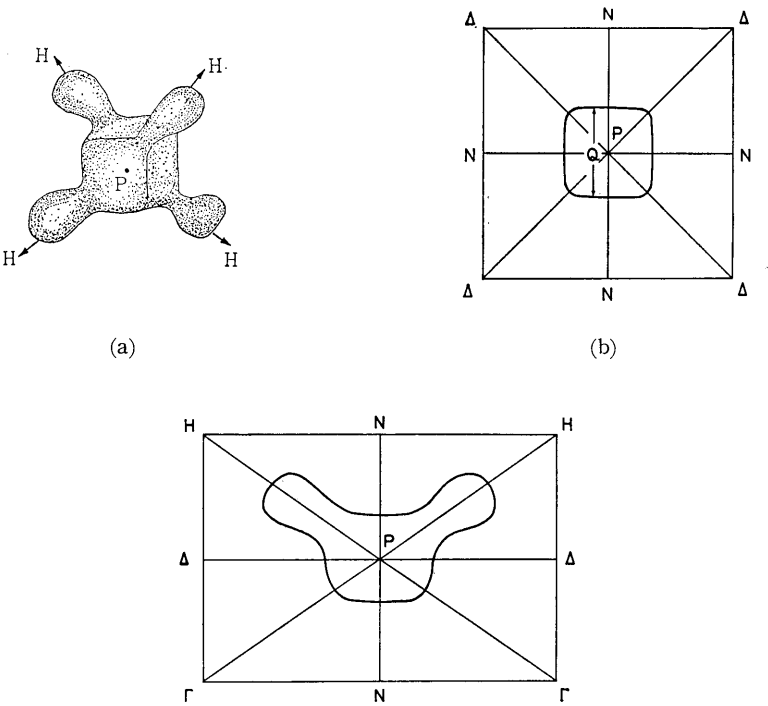

Fig. 4. (a) Our hole Fermi surface ($\alpha=1$). ($E_F=0.225$ Ry).
(b) Cross-section in the PNN′-plane [(100)-plane].
(c) Cross-section in the PNH-plane [(110)-plane].

the latter since the latter has four large wings. Thus, if the form of the electron Fermi surface is "cube"-like such as "superegg", we might feel simply that "superegg" should play an essential role for the HSO rather than "tetracube", i. e., the HSO in bcc Eu should occur by the pitch-vector 2Q rather than Q. But, the observed fact is contrary to the above expectation. This fact leads us to the conviction that the form of the electron Fermi surface will not be "cube"-like.

With a purpose to solve this problem, we (1976; 1977) calculated the detailed Fermi surface by the KKR method by using the $X\alpha$-exchange potential of $\alpha=1$. Our results of calculation were as follows.

Our hole surface around P had quite resemblance to ANDERSEN and LOUCKS' "tetracube". Our hole surface and its cross-section in the PNN'-[(100)-] and PNH-[(110)-] planes are shown in Fig. 4.

But, as for the electron surface shape, our calculating result was somewhat much rounder than ANDERSEN and LOUCKS' "superegg". Our electron surface (tentatively named as "bumpy sphere") and its cross-section in the HΓN-[(100)-] and HΓP-[(110)-] planes are shown in Fig. 5. From this "sphere"-like shape of Fig. 5, we understood the reason why the electron Fermi surface does not play

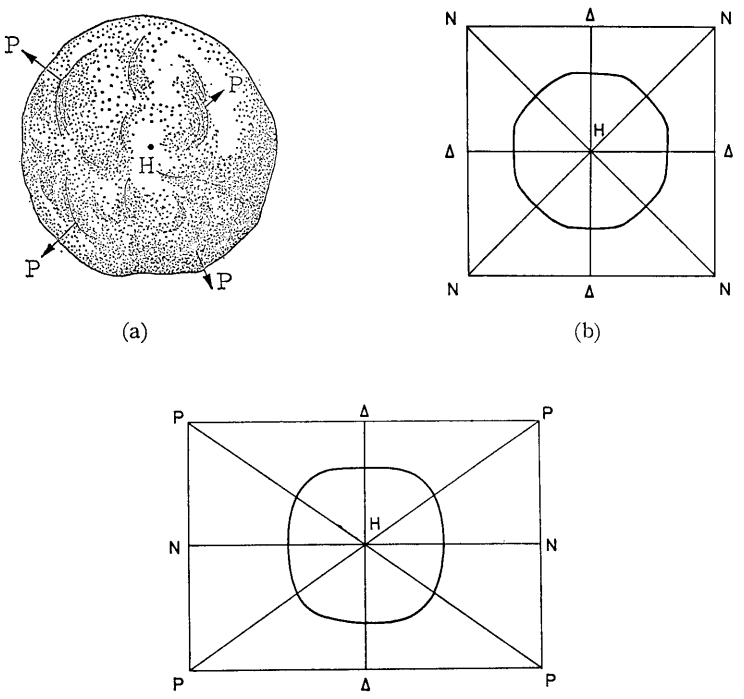

Fig. 5. (a) Our electron Fermi surface: "bumpy sphere" ($\alpha=1$). ($E_F=0.225$ Ry).
(b) Cross-section in the HΓN-plane [(100)-plane].
(c) Cross-section in the HΓP-plane [(110)-plane].

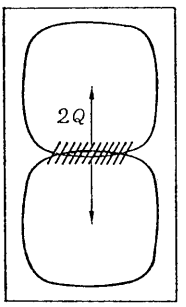

Fig. 6. One edge "nesting" into the opposite one in "superegg".

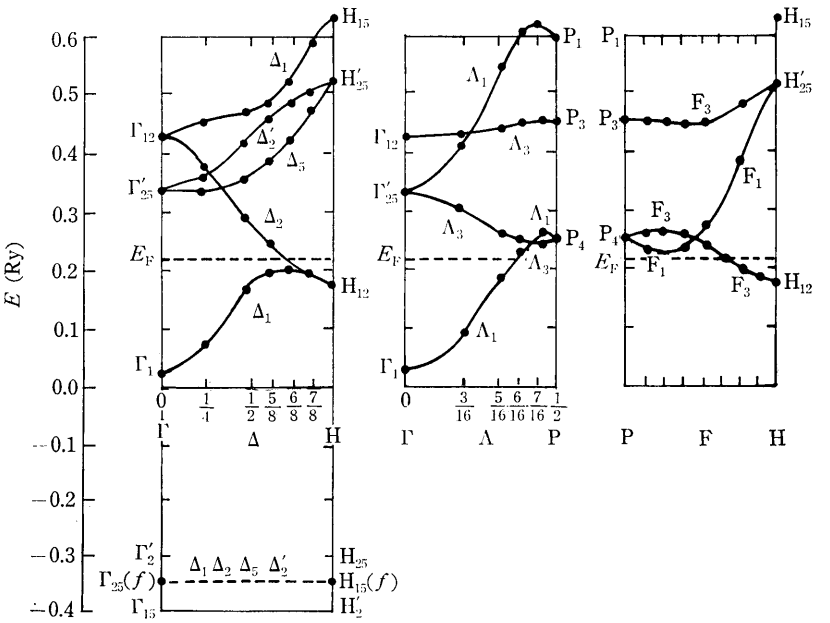

Fig. 7. Energy band structure of bcc Eu along the three symmetry axes ($\alpha=1$; ours (1976; 1977)).

almost any role for the HSO, because, for ours, there will be no one-edge-nesting into the opposite one (cf. Fig. 6 for the nesting in the case of "superegg").

Our band structure along the symmetry lines Γ-Δ-H, Γ-Λ-P, and P-F-H for $\alpha=1$ are shown in Fig. 7. Width of d-band (H_{12} to H'_{25}) and that of sp-band (Γ_1 to H_{15}) are 0.35 Ry and 0.61 Ry, respectively. Both these values and band-structure-form along the symmetry lines have a strong resemblance to FREEMAN and DIMMOCK (1966). It is also to be noted that the very narrow $4f$-bands (width=

0.008 Ry) are located considerably below the condunction bands, i. e., at about -0.37 Ry below the bottom of the conduction bands, for this case of $\alpha=1$.

§ 2. Crystal Potentials for $\alpha=2/3$, 0.8, 0.9, and 1

In the previous papers (1976; 1977), our muffin-tin-potential V_{mt} ($\alpha=1$) in bcc Eu was made up for the configuration $4f^7 5d^0 6s^2$ by using HERMAN and SKILLMAN's self-consistent-field Hartree-Fock-Slater (SCF-HFS) AO's of $\alpha=1$ (1963) on the basis of the renormalized atomic model. This V_{mt}, having the $\alpha=1$ exchange-potential, is consistent with the adopted AO's ($\alpha=1$).

Now, we have made the similar calculations for the values of $\alpha=2/3$, 0.8, and 0.9 as the previous value of $\alpha=1$. The most essential point is that we have to use the SCF-HFS AO's with the same α-value as a crystal potential which we should like to construct.

Several sets of SCF-HFS AO's are, then, prepared for $\alpha=2/3$ (WAKOH; 1978); $\alpha=0.8$ (WAKOH; 1978); and $\alpha=0.9$ (Ours; 1979). From these material-AO-sets, we have constructed several new crystal potentials V_{mt} ($\alpha=2/3$), V_{mt} ($\alpha=0.8$), V_{mt} ($\alpha=0.9$), and V_{mt} ($\alpha=$mix), all using the same electron configuration $4f^7 5d^0 6s^2$ as in the case of SLATER's $X\alpha$-type exchange potentials

$$V_{\text{exch}}(\boldsymbol{r})=-6\alpha\left[\frac{3}{8\pi}\rho_{\text{crys}}(\boldsymbol{r})\right]^{1/3}\ (\text{Ry}) \qquad (1)$$

which are made up by the above mentioned SCF-HFS-AO's for $\alpha=2/3$, $\alpha=0.8$, and $\alpha=0.9$, respectively. On the other hand, the last V_{mt} ($\alpha=$mix) was made up by the following way. The value of α in eq. (1) was taken as 2/3, but $\rho_{\text{crys}}(\boldsymbol{r})$ in eq. (1) was constructed by making use of HERMAN-SKILLMAN's ($\alpha=1$) SCF-HFS-AO's. This V_{mt} ($\alpha=$mix) was found to give preposterous questionable band structure, especially for $4f$-bands, so that we discard it hereafter.

Other points for constructing our muffin-tin-potentials are quite similar to those mentioned in our previous paper (1977).

§ 3. Band Structures and Fermi Surfaces for $\alpha=2/3$, 0.8, and 0.9

It has been established by CONNOLLY (1967) that the energy bands in ferromagnetic $3d$-metals in the case of $\alpha=1$ give results in qualitative disagreement with experiments, whereas reducing the exchange to $\alpha=2/3$ gives good agreement for most of the experimental data, especially for those data which are strongly related to the Fermi surface structure such as de Haas-van Alphen and magneto-resistance experiments.

In view of the situation, we now have a plan to calculate the band structures, the Fermi energies, and the detailed structures of the Fermi surface for the above three values of α, in addition to $\alpha=1$. The Γ-Δ-H band structures obtained and the values of the Fermi energy determined for the four α's are shown in

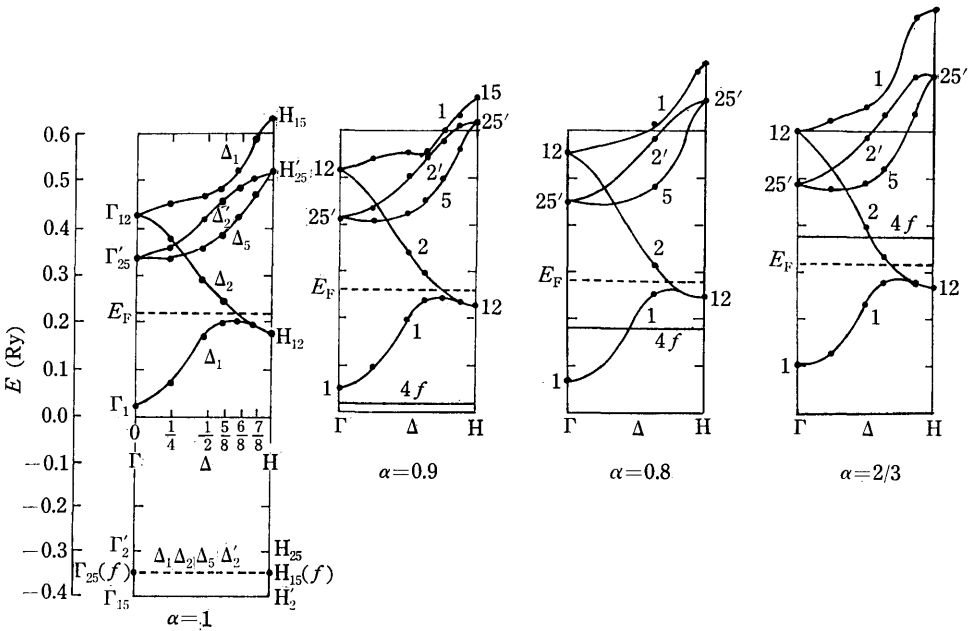

Fig. 8. Comparison of the band structures along the Γ-Δ-H axis for $\alpha=2/3$, 0.8, 0.9, and 1.

Table 1. Fermi energy values E_F (Ry) of bcc Eu for $\alpha=2/3$, 0.8, and 0.9 determined by our present calculations.

α	$\varepsilon_F^{(*)}$	E_F (Ry)	Error (%)
2/3	0.600	0.317	4.1
0.8	0.552	0.292	1.2
0.9	0.514	0.271	3.4
1.0	0.427	0.225	4.3

* $\varepsilon=(a/2\pi)^2E$

Fig. 8 and Table 1, respectively. In Fig. 8, we can see that both E_F and $4f$-band position are raised as the α-value decreased*. The $4f$-bands (levels) are located below the conduction bands for $\alpha=1$ and 0.9, and in the middle part of the occupied conduction bands for $\alpha=0.8$, and above the Fermi energy for $\alpha=2/3$. But, here, it should be noticed that the width of the $4f$-bands (levels) still is found to be very narrow (<0.02 Ry) even in $\alpha=2/3$. In Table 1, ε is an enery

* In the case of $\alpha=2/3$, we notice that the energy eigenvalues of the $4f$-bands become to locate a little above the Fermi energy E_F, where E_F means the Fermi energy for the configuration $(4f)^7$ (c. e.)^2 [c. e.=conduction electron]. This problem will be discussed in near future.

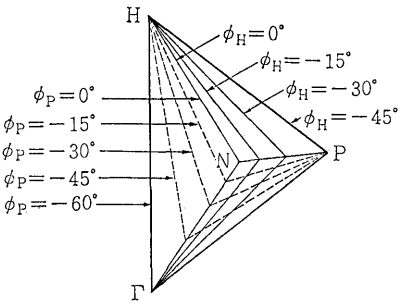

Fig. 9. Nine cross-sections on which we have calculated the electron surface around H and the hole surface around P.

parameter defined as

$$\varepsilon=(a/2\pi)^2E \qquad (2)$$

where E is the energy eigenvalue in Rydberg.

The Fermi energy E_F for every α-value has been determined within the error shown in the last column in Table 1. The procedure and the meaning of the error are as follows.

We calculate the electron Fermi surface around H, and the hole surface around P, in the 1/48 Brillouin zone (BZ) shown in Fig. 1. In calculating the electron surface, spherical coordinates are taken with the origin at H, the z-axis along the edge HΓ, and the azimuthal angle $\phi_H=0°$ and $-45°$ as the planes HΓN and HΓP, respectively (Fig. 9).

On the other hand, for the hole surface, we also use spherical coordinates with the origin at P, the z-axis along PH, and the planes $\phi_P=0°$ and $-60°$ as the planes PHN and PHΓ, respectively.

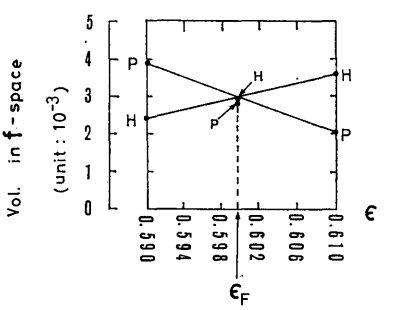

Fig. 10. Method for determination of the Fermi energy parameter ε_F in the case of $\alpha=2/3$. (We have used the similar methods for the other values of α.)

We define dimensionless $\boldsymbol{f}$-vector as

$$\boldsymbol{f}=(a/2\pi)\boldsymbol{k} \tag{3}$$

and if we let V(H) and V(P) be the electron volume around H and the hole volume around P in the 1/48 BZ in the $\boldsymbol{f}$-space, the relation

$$\mathrm{V(H)}=\mathrm{V(P)} \tag{4}$$

has to be satisfied, since bcc Eu is a compensated metal.

As an example, our way of determination of the Fermi energy in the case of $\alpha=2/3$ is shown in Fig. 10. First, we have tried the value $\varepsilon=0.590$, and we have obtained the result V(P)>V(H), as shown in Fig. 10. Then, we have tried $\varepsilon=0.610$, and we have got V(H)>V(P). By connecting both V(H)-points and both V(P)-points on the graph by straight lines, we have the cross-point which corresponds to $\varepsilon=0.600$ ($E=0.317$ Ry).

Next, we have again calculated V(H) and V(P) for $\varepsilon=0.600$, and have got

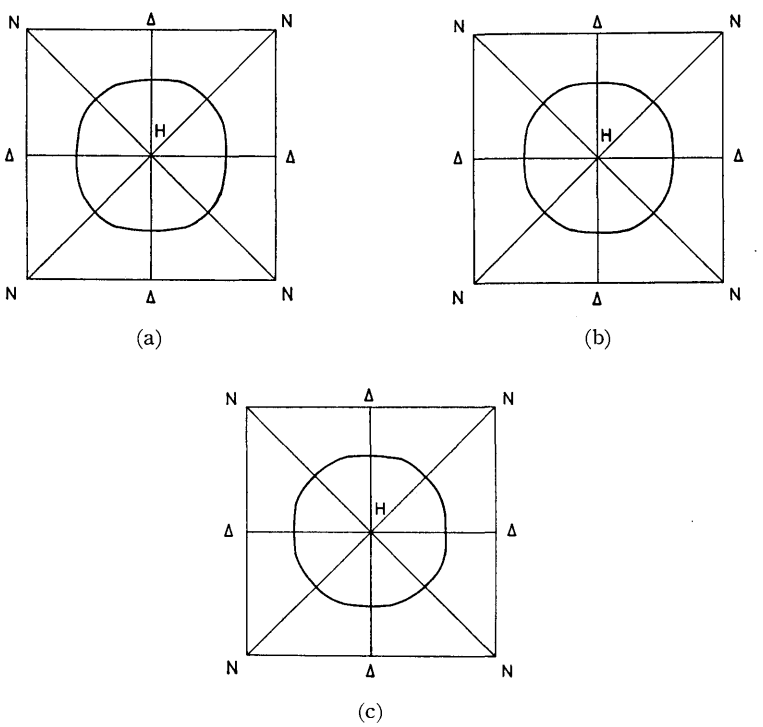

Fig. 11. HΓN-[(100)-] cross-sections of our electron Fermi surface around H, in the cases of

(a) $\alpha=2/3$ ($E_F=0.317$ Ry),
(b) $\alpha=0.8$ ($E_F=0.292$ Ry), and
(c) $\alpha=0{\cdot}9$ ($E_F=0.271$ Ry).

$V(H)=0.294\times10^{-2}$, and $V(P)=0.282\times10^{-2}$, so that

$$\frac{V(H)-V(P)}{V(H)}=4.1\% \qquad (5)$$

The value of (5) is shown in the last column of Table 1, as well as the ones for other α-values.

Now, as the results of the present calculation, we shall show the detailed forms of the electron Fermi surface and the hole Fermi surface for the above mentioned four values of α.

First, in Fig. 11, the (100)-cross-sections (HΓN-planes) of the electron surface around H are shown for $\alpha=2/3$, 0.8, and 0.9. These are compared with our previous result of Fig. 5 (b) for $\alpha=1$ and ANDERSEN and LOUCKS' result of Fig. 2 (b). As is easily seen, Fig. 11 (a), (b), (c) and Fig. 5 (b) are quite similar in form, and all of them are "circle"-like. On the other hand, Fig. 2 (b) is rather "square"-like.

Secondly, in Fig. 12, the (110)-cross-sections (HΓP-planes) of the same electron surface are shown also for $\alpha=2/3$, 0.8, and 0.9. These are compared with our previous result of Fig. 5 (c). They have all quite resemblance in form, and we

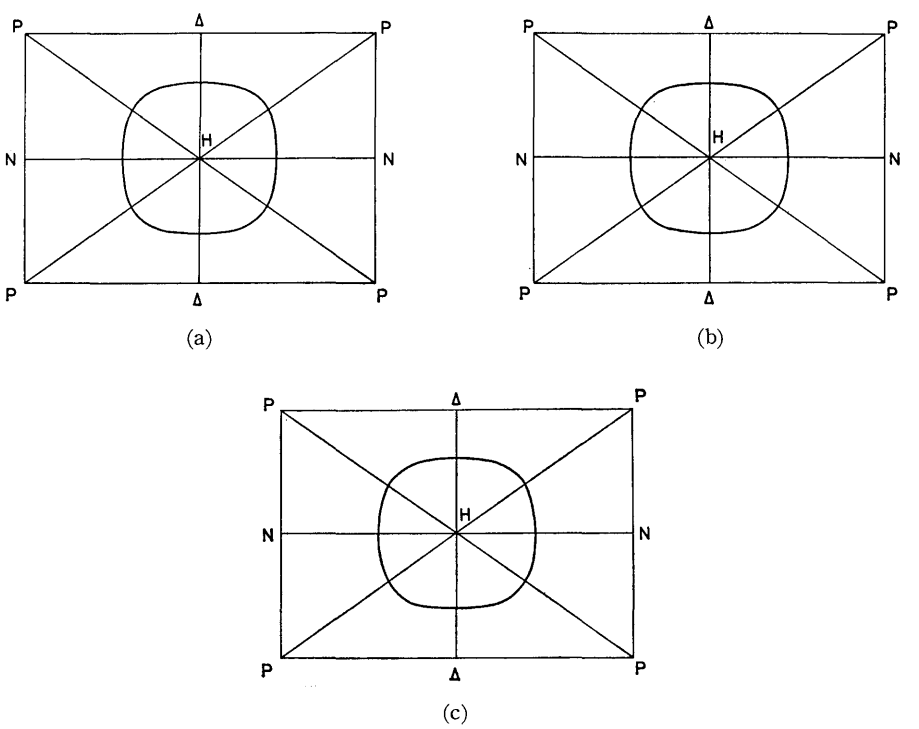

Fig. 12. HΓP-[(110)-] cross-sections of our election Fermi surface around H, in the cases of (a) $\alpha=2/3$, (b) $\alpha=0.8$, and (c) $\alpha=0.9$.

may easily imagine that our electron Fermi surface ("bumpy sphere") has eight small mounds near the directions from central H to eight P's, for every value of α.

Thirdly, in Fig. 13, the (100)-cross-sections (PNN'-planes) of the hole Fermi surface around P are shown for the same three α-values. They all quite resemble each other and with Fig. 4 (b) of our previous result of $\alpha=1$, and moreover, the magnitude $[0.33(2\pi/a)]$ of the Q-vector shown in Fig. 4 (b) agrees very well with those in Fig. 13 (a), (b), and (c). We can understand that the nesting due to this Q-vector explains the HSO $[Q=0.29(2\pi/a)]$ shown experimentally by NERESON et al. (1964) for bcc Eu.

Lastly, in Fig. 14, the (110)-cross-sections [PNH-planes] are shown for the same α-values. These are also quite similar to our previous result Fig. 4 (c) for $\alpha=1$. Then, as far as the hole surface is concerned, the form of "tetracube" (Fig. 3) given by ANDERSEN and LOUCKS (1968) and our previous form (Fig. 4 (a)) resemble qualitatively, and on the whole, there will be no difference between them (except the form of the cross-section of the tetrahedrally located wings perpendicular to the PH-axis (cf. our paper (1976)).

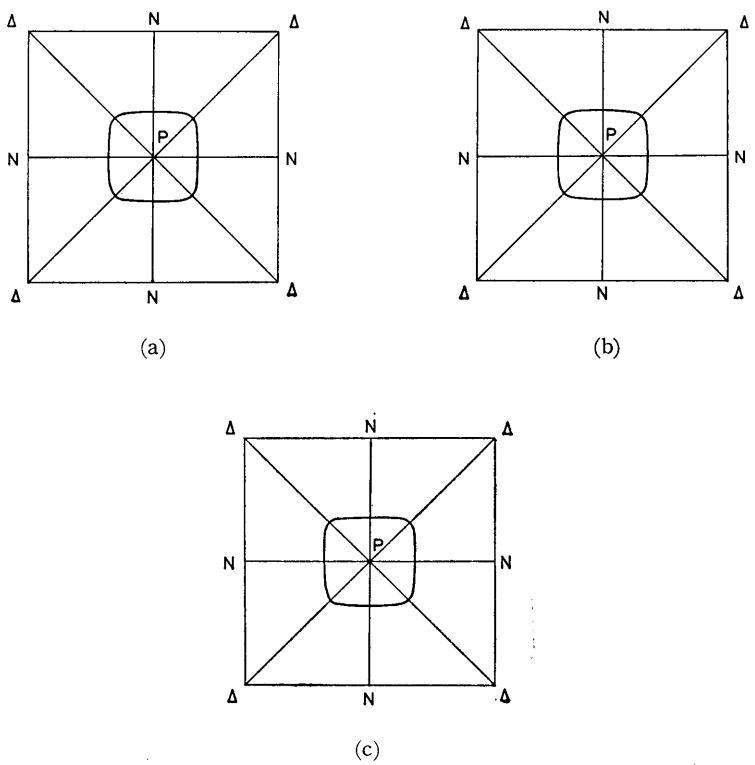

Fig. 13. PNN'-[(100)-] cross-sections of our hole Fermi surface around P, in the cases of (a) $\alpha=2/3$, (b) $\alpha=0.8$, and (c) $\alpha=0.9$.

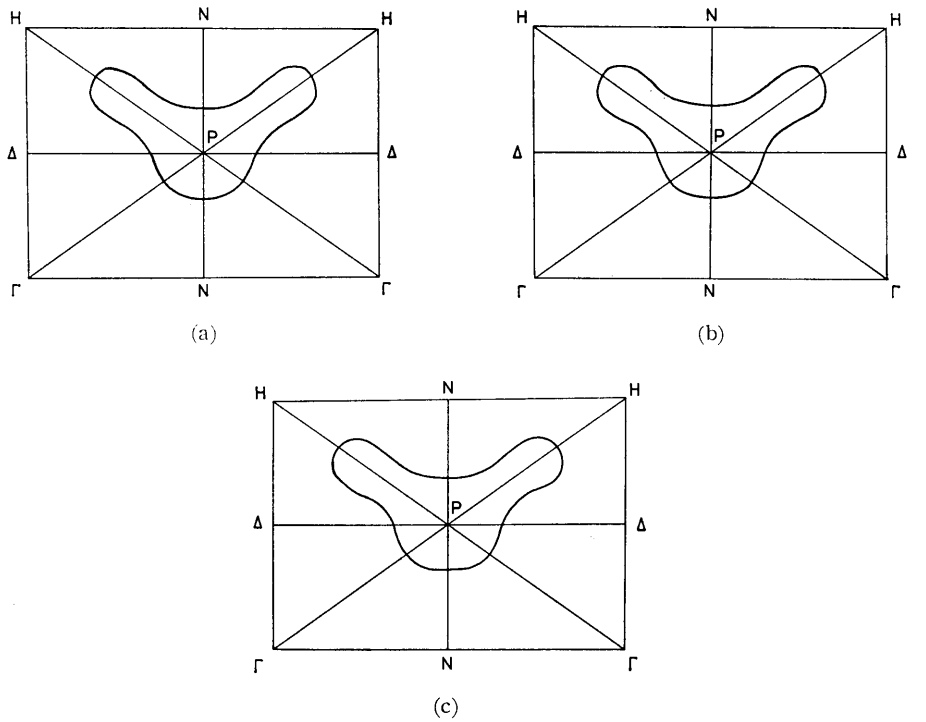

Fig. 14. PNH- [(110)-] cross-sections of our hole Fermi surface around P, in the cases of (a) $\alpha=2/3$, (b) $\alpha=0.8$, and (c) $\alpha=0.9$.

§ 4. Conclusion

From our present calculations for the detailed forms of the electron and hole Fermi surfaces of bcc Eu, we may suppose we can bring out the following important conclusions.

(1) The form of the electron Fermi surface is rather "sphere"-like as shown in Fig. 5 ("bumpy sphere"), and not "cube"-like shown in Fig. 2(a) ("superegg"). Thus, it may safely be considered that the electron Fermi surface does not contribute to the helical spin ordering (HSO) of bcc Eu.

(2) The form of the hole Fermi surface is shown in Fig. 3 ("tetracube") and in Fig. 4(a). There is no essential difference between them (except the form of the cross-section of the tetrahedrally located wings as shown in Fig. 7 of our previous paper (1976)). The hole Fermi surface does contribute to the HSO of bcc Eu.

Finally, the authors should like to express their sincere gratitude to Professor A. J. FREEMAN for his helpful advices. They also wish to thank Dr. S. WAKOH for providing them with the SCF-HFS-AO's for $\alpha=2/3$ and 0.8. The numerical

calculations were made with the kind assistance of Mr. K. HIURA and the members of the Computer Center of Nihon University at Setagaya in Tokyo, and performed mainly at the Computer Center of Tokyo University.

REFERENCES

OLSEN, C. E., NERESON, N. G. and ARNOLD, G. P. (1962): Neutron Diffraction Studies on Europium Metal, J. Appl. Phys. Suppl., **33**, 1135–1136.

NERESON, N. G., OLSEN, C. E. and ARNOLD, G. P. (1964): Magnetic Structure of Europium, Phys. Rev., **135**, A 176–A 180.

FREEMAN, A. J. and DIMMOCK, J. O. (1966): Band Structure and Electronic Properties of Europium Metal, Bull. Amer. Phys. Soc., **11**, 216; and unpublished data.

ANDERSEN, O. K, and LOUCKS, T. L. (1968): Fermi Surface and Antiferromagnetism in Europium Metal, Phys. Rev. **167**, 551–556.

KOBAYASI, S.-I., FUKUCHI, M. and NAGAI, S. (1973): Numerical Calculation of Isomer Shift on Eu^{151}, Solid State Commun., **13**, 727–732.

KOBAYASI, S.-I., FUKUCHI, M. and NAGAI, S. (1976): Fermi Surface and Helical Spin Ordering in Eu Metal, Solid State Commun., **20**, 589–593.

KOBAYASI, S.-I., FUKUCHI, M. and NAGAI, S. (1977): Band Structure and the Fermi Surface of Rare Earth Metal Europium, Physica, **86–88 B**, 26–27.

CONNOLLY, J.W.D. (1967): Energy Bands in Ferromagnetic Nickel, Phys. Rev. **159**, 415–426.

WAKOH, S. (1978): private communications.

MATSUMOTO, M., SHIBATA, I., FUKUCHI, M., SAKIZI, Y. and KOBAYASI, S.-I. (1979): unpublished data.

HERMAN, F. and SKILLMAN, S. (1963): "Atomic Structure Calculations", (Prentice-Hall, Inc.).